

Bias polarity-dependent unipolar switching behavior in $NiO/SrTiO_3$ stacked layer

Xian-Wen Sun(孙献文), Cai-Hong Jia(贾彩虹), Xian-Sheng Liu(刘献省), Guo-Qiang Li(李国强), Wei-Feng Zhang(张伟风)

Citation: Chin. Phys. B . 2018, 27(4): 047304. **doi:** 10.1088/1674-1056/27/4/047304

Journal homepage: http://cpb.iphy.ac.cn; http://iopscience.iop.org/cpb

What follows is a list of articles you may be interested in

Novel hole transport layer of nickel oxide composite with carbon for high-performance perovskite solar cells

Sajid, A M Elseman, Jun Ji(纪军), Shangyi Dou(窦尚轶), Hao Huang(黄浩), Peng Cui(崔鹏), Dong Wei(卫东), Meicheng Li(李美成)
Chin. Phys. B . 2018, 27(1): 017305. **doi:** 10.1088/1674-1056/27/1/017305

Effect of metal catalyst on the mechanism of hydrogen spillover in three-dimensional covalent-organic frameworks

Xiu-Ying Liu(刘秀英), Jing-Xin Yu(于景新), Xiao-Dong Li(李晓东), Gui-Cheng Liu(刘桂成), Xiao-Feng Li(李晓凤), Joong-Kee Lee
Chin. Phys. B . 2017, 26(2): 027302. **doi:** 10.1088/1674-1056/26/2/027302

Charge susceptibilities of armchair graphene nanoribbon in the presence of magnetic field

H Rezania, F Azizi
Chin. Phys. B . 2016, 25(9): 097303. **doi:** 10.1088/1674-1056/25/9/097303

Structural, electronic, and magnetic properties of transition-metal atom adsorbed two-dimensional GaAs nanosheet

Jia Luo(罗佳), Gang Xiang(向钢), Tian Yu(余天), Mu Lan(兰木), Xi Zhang(张析)
Chin. Phys. B . 2016, 25(9): 097305. **doi:** 10.1088/1674-1056/25/9/097305

Structures and electrical properties of pure and vacancy-included ZnO NWs of different sizes

Yu Xiao-Xia, Zhou Yan, Liu Jia, Jin Hai-Bo, Fang Xiao-Yong, Cao Mao-Sheng
Chin. Phys. B . 2015, 24(12): 127307. **doi:** 10.1088/1674-1056/24/12/127307

Bias polarity-dependent unipolar switching behavior in $NiO/SrTiO_3$ stacked layer*

Xian-Wen Sun(孙献文), Cai-Hong Jia(贾彩虹), Xian-Sheng Liu(刘献省), Guo-Qiang Li(李国强), and Wei-Feng Zhang(张伟风)†

Henan Key Laboratory of Photovoltaic Materials and School of Physics and Electronics, Henan University, Kaifeng 475004, *China*

(Received 18 September 2017; revised manuscript received 22 January 2018; published online 10 March 2018)

The identification of the switching location has been a key technology to tune the physical properties of unipolar resistive switching (RS) cells. Here we report the RS properties of Au/NiO/$SrTiO_3$(STO)/Pt memory cells. The switching repeatability is closely related to the applied bias polarity, which is different from the scenario of the Au/STO/Pt cells reported in our previous researches. The high resistance in positive bias is greater than that in negative bias. The $R(T)$–$R_0I^2R(T)$ plot of the on-state I–V curve shows a regular shape only with a slight bend and an abnormal shape with an abrupt increase and decrease under negative and positive bias, respectively. These comparative experimental results reveal that the conductance filament consisting of oxygen vacancies grows from the cathode to the anode. The spatial RS location is identified with the weaker part along the conductance filament length direction, which should be near the NiO/STO interface and STO/Pt interface under positive and negative bias, respectively.

Keywords: $SrTiO_3$ thin film, unipolar resistive switching, oxygen vacancies

PACS: 73.22.–f, 73.50.–h **DOI:** 10.1088/1674-1056/27/4/047304

1. Introduction

Resistive random access memory (RRAM) is one of the most promising candidates for emerging nonvolatile memory, which is based on resistive switching (RS) between a high resistance state (HRS) and a low resistance state (LRS) under external electric stimulus.[1–3] The RS behavior has been intensively investigated in a large variety of oxide materials, including binary and perovskite-type oxides.[2–5] For unipolar RS, i.e., where the switching can be induced by an applied bias with the same polarity, the RS originates from the formation and rupture of nanometer-scale conducting filaments in the oxide layer.[6,7] From a microscopic point of view, the conductance filaments (CFs) are formed or ruptured in the nanoionic transport and redox reaction processes triggered by an electric field or temperature or both.[8] In oxides-based RS devices, the oxygen vacancy (ion) migration under an external electric field is an essential factor affecting the formation and rupture of CFs.[7–10] The reported work showed that unipolar RS has several merits, such as high-density, large off/on resistance ratio (10^3–10^6), and simpler design for drive circuits. However, there are still several key concerns including the inappropriate repeatability of the RS parameter and insufficient endurance, which are obstacles to realize the RRAM as a practical technology.[10–13] The commonly accepted opinion about the non-uniform RS performances with increasing the number of RS cycles is related to the non-uniform and uncontrolled formation and rupture of CFs over a large area of the memory cell, which is caused by their random nucleation and uncontrolled growth. Hence, we believe that it would be advantageous to define the location of the filamentary RS and growing direction of CFs to improve the performances of filamentary RS.

Previously, we reported that the unipolar RS behaviors independent of bias polarity were observed in Au/$SrTiO_3$/Pt memory cells with 10-mA compliance current (CC).[14] Because it is difficult to achieve spatial information within a single layer RS material, we introduce NiO thin films between Au and $SrTiO_3$ (STO) films in this work. The Au/NiO/STO/Pt cells exhibit unipolar RS, and the switching repeatability is closely related to the applied bias polarity. The spatial switching location and growing direction of CFs are further investigated based on the experimental results.

2. Experimental section

NiO and STO thin films were layers deposited on (111) Pt substrates by the pulsed laser deposition technique. A pulsed KrF excimer laser (COMPexPro201, Coherent) with a wavelength of 248 nm, pulse duration of 25 ns, frequency of 5 Hz, and a lens with a focal length of 300 mm was focused on the sintered ceramic targets with a purity of 99.99%. The STO and NiO films were deposited at substrate temperatures of 700 °C and 600 °C, respectively, and the oxygen pressure of 12 Pa re-

*Project supported by the National Natural Science Foundation of China (Grant No. 11404093), the Foundation of Henan Provincial Science and Technology Department, China (Grant No. 132102210258), the Research Funding from Henan Province, China (Grant Nos. 15A140001, 2015GGJS-021, and 17HASTIT014), and the Henan University Emerging Cross and Characteristic Discipline Cultivation Program, China (Grant No. xxjc20140016).

†Corresponding author. E-mail: wfzhang@henu.edu.cn

© 2018 Chinese Physical Society and IOP Publishing Ltd

mained unchanged. The nominal thickness values of NiO and STO films are about 100 nm and 400 nm, respectively, which can be determined according to the cross-sectional SEM image and energy dispersive x-ray spectra as shown in Figs. 1(a) and 1(b)). Then the 100-nm thick Au top electrode with a diameter of 100 μm was sputtered onto an as-deposited NiO/STO stacked film through a shadow mask by dc sputtering. The cell structure and electrical measurement schematic is shown in the inset of Fig. 2(a), in which the current and voltage are measured by a Keithley 2400 SourceMeter on the same two electrodes. A bias that drives current flowing from NiO to STO film is defined as being positive.

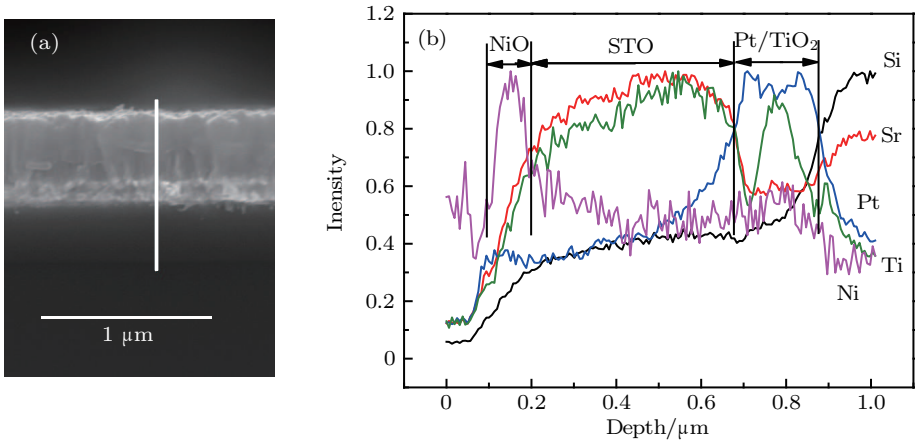


Fig. 1. (color online) (a) Cross-sectional SEM image of the NiO/STO thin film on Pt/TiO_2/SiO_2/Si substrate. (b) Energy dispersive x-ray spectra (EDS) for NiO/STO films on Pt/TiO_2/SiO_2/Si substrates, which exhibits atomic concentrations of four elements (Ni, Ti, Sr, and Si) with depth profiling. This figure demonstrates that thickness values of NiO and STO films are about 100 nm and 400 nm, respectively. Peak of Ti element between 0.7 μm and 0.9 μm represents TiO_2 in Pt/TiO_2/SiO_2/Si substrate.

3. Results and discussion

Figure 2(a) displays the *I*–*V* curves of the pristine Au/NiO/STO/Pt memory cell. The original resistance of this cell is large due to the presence of interface barriers, which can be identified by the rectifying *I*–*V* curves. It is well known that NiO is a p-semiconductor with Ni^{2+} vacancies formed by the nickel deficit, which provide holes for the valence band,[15] and STO is an n-semiconductor with oxygen vacancies which provide electrons for the conduction band.[16] So, p–n junctions are formed at the NiO/STO heterojunction interface, which brings about the unidirectional conduction characteristics under positive bias. Normally, an electroforming process is required to obtain conductance and activate reversible and reproducible RS behavior for a memory cell with high resistance. In the present work, the electroforming processes are completed in two steps. The first step is that a gradually increasing negative bias is applied until the current jumped to the compliance level of 1 mA as shown in the inset of Fig. 2(b). The current jump occurs at about 14 V for this cell. The second step is a voltage sweep with 10-mA CC under smaller bias range as shown in Fig. 2(b). Three repetitive *I*–*V* curves in a bias range of ±3 V show that the currents gradually decrease and become smooth with the bias scanning. The corresponding currents further decrease when the bias increases from ±3 V to ±5 V. After that, the rectification observed in the pristine state disappears and nearly symmetric *I*–*V* curves are seen. This indicates that the high density defect within the active thin film matrix is created under strong electrical stress, which is associated with the fact that oxygen-vacancy migration (or oxygen diffusion) is significantly enhanced along extended defects.

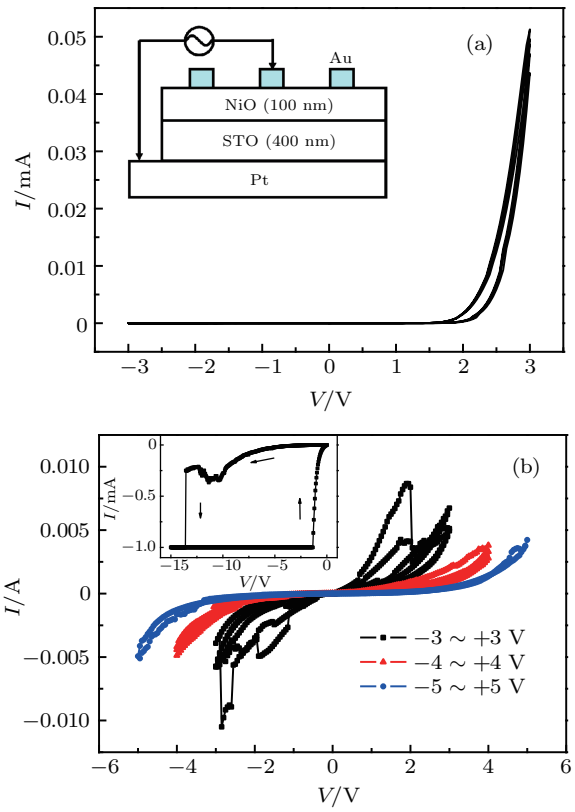


Fig. 2. (color online) (a) Rectifying *I*–*V* curves in pristine Au/NiO/STO/Pt memory cell. Inset shows the schematic drawing of the *I*–*V* measurement. (b) Voltage sweep with 10-mA CC in smaller voltage range. Inset shows electroforming process with 1-mA CC under negative bias.

After electroforming, the Au/NiO/STO/Pt memory cells present unipolar RS behaviors, where the CC is controlled at 10 mA. Interestingly, the switching repeatability has strong dependence on the bias polarity. The cell shows reliable and repeatable unipolar RS under a negative bias as shown in Fig. 3(a). However, under a positive bias, this cell only displays a few switching cycles (about 4–7 cycles) and soon reaches the non-switching state irrespective of the CC (as shown in Fig. 3(b)). The inset in Fig. 3(c) exhibits the *I*–*V* curve of the last cycle, in which the cell remains in HRS and becomes higher at about 24 V. After this, the Au/NiO/STO/Pt cell cannot be recovered to the RS possible state even with 30 V bias as shown in Fig. 3(c). Moreover, the occurrence of the non-switching state is independent of the order of the positive or negative bias. If positive bias is applied to the cell after the electroforming process, the non-switching state is still observed after the RS has performed a few times (shown in Fig. 3(d)). This result is the same as that in Fig. 3(c). It should be noted that the Au/STO/Pt cells exhibit unipolar RS behaviors independent of bias polarity, which was shown in our previous work.[14] So, it can be deduced that such a bias polarity dependent unipolar RS behavior in Au/NiO/STO/Pt cells is closely related to the introduction of NiO film.

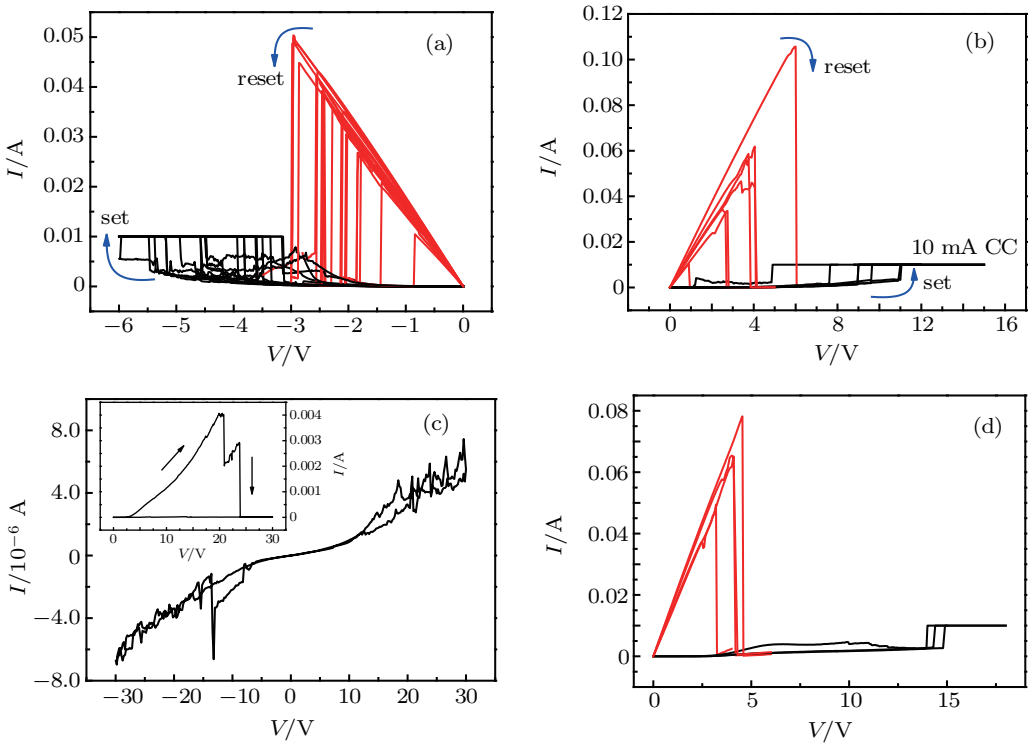


Fig. 3. (color online) (a) Repeated unipolar RS characteristics of Au/NiO/STO/Pt cell under negative bias. (b) Under positive bias the cell just shows a few switching cycles (about 4–7 cycles). Inset in panel (c) exhibits *I*–*V* curve of the last cycle, in which high resistance becomes higher at about 24 V. After this, the Au/NiO/STO/Pt cell cannot be recovered to the RS possible state even with 30-V bias as shown in panel (c). (d) If positive bias is applied to the cell after the electroforming processes, the non-switching state is still observed after RS has been performed a few times.

Figure 4 shows the resistance values of HRS and LRS under positive and negative bias, which are extracted from Figs. 3(a) and 3(b). There is no obvious difference in LRS, while the high resistance under positive bias is greater than that under negative bias. The high resistance values under negative and positive bias are within the ranges of 10^4 Ω–10^5 Ω and 10^5 Ω–10^6 Ω, respectively. Because the repeated unipolar RS originates from the formation and rupture of CFs, the current in HRS is distributed homogeneously across the cell area, and the current in LRS is localized to CFs.[7,17] So in this work, the different HRSs under positive and negative bias indicate that the bulk resistance of the NiO/STO stacked layer is affected by the bias polarity.

Comparing both types of reset switching curves in Figs. 3(a) and 3(b), the on-state *I*–*V* curves (i.e. curves in LRS) generally show Ohmic behaviors (i.e., linear *I*–*V*) in the low voltage region, indicating the metallic nature of CFs. However, the *I*–*V* curves each deviate from the linear shape in the high voltage region, which is due to the Joule heating effect that changes the Ohmic behaviors of CFs.[18] For a better understanding of the polarity-dependent unipolar RS in Au/NiO/STO/Pt cells, we investigate the relationship between the filament resistance and the Joule heating. Supposing that R_0 is the filament resistance at room temperature, γ is the temperature coefficient of resistance, which is the intrinsic characteristic of an RS material, and ΔT is the temperature change

in the filament, the filament resistance R, which will change due to the Joule heating effect, can be represented as follows:

$$R = R_0[1 + \gamma(\Delta T)]. \quad (1)$$

The reset behavior originates due to the partial rupture of the metallic CFs by Joule heating. Lee *et al.* recently reported that ΔT in Eq. (1) is proportional to the power, specifically, I^2R ($\Delta T = KI^2R(T)$),[19] where K is a coefficient. Therefore, equation (1) could be rewritten as

$$R(T) = R_0[1 + \gamma K I^2 R(T)] = R_0 + \gamma K R_0 I^2 R(T). \quad (2)$$

In Eq. (2), γ is the intrinsic characteristic of an RS material, and K is related to both the intrinsic property of a material such as heat capacitance of filament material, and the filament shape factor such as filament surface area for heat dissipation.

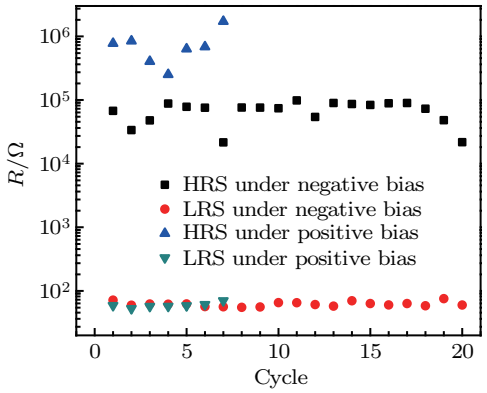


Fig. 4. (color online) Resistance values versus cycle of HRS and LRS under negative and positive bias, which are extracted from Figs. 2(a) and 2(b). Read voltage is 0.1 V.

According to Eq. (2), the slope of the $R(T)$–$R_0I^2R(T)$ plot provides information about the γK value in each RS material system. For a given material system, γ is constant while K depends on R_0 because the CF resistance is related to the shape and size of the CF.[18] The accurate quantitative relationship between K and R_0 is difficult to determine at this point. However, the slope of the $R(T)$–$R_0I^2R(T)$ plot, which corresponds to the γK value, must be specific for each RS material system. Therefore, this type of plot can give a better indication of the material portion where RS actually occurs than the original switching I–V curves shown in Fig. 3.

Figure 5 shows the $R(T)$–$R_0I^2R(T)$ plots of the on state I–V curves (V region up to the point immediately before reset occurs in Figs. 3(a) and 3(b)). In this type of plot, the graph generally has a linear shape in the low V region, suggesting constant material properties, but deviates from linearity before reset occurs due to the structural modification of the CF at this point. Therefore, an examination of the change in linear shape can provide clearer evidence where the reset switching occurs. The $R(T)$–$R_0I^2R(T)$ plot shows a regular shape only with a slight bend, and an abnormal shape with an abrupt increase and decrease under negative and positive bias, respectively as shown in Figs. 5(a) and 5(b). The slight deviation from the linear curve may be caused mainly by the changed filament resistance due to the Joule heating effect, but the abrupt increase and decrease should be induced not only by the Joule heating effect. We can deduce that the reset switching occurs in the same material under negative bias, but the CFs are ruptured within different material regions under positive bias.

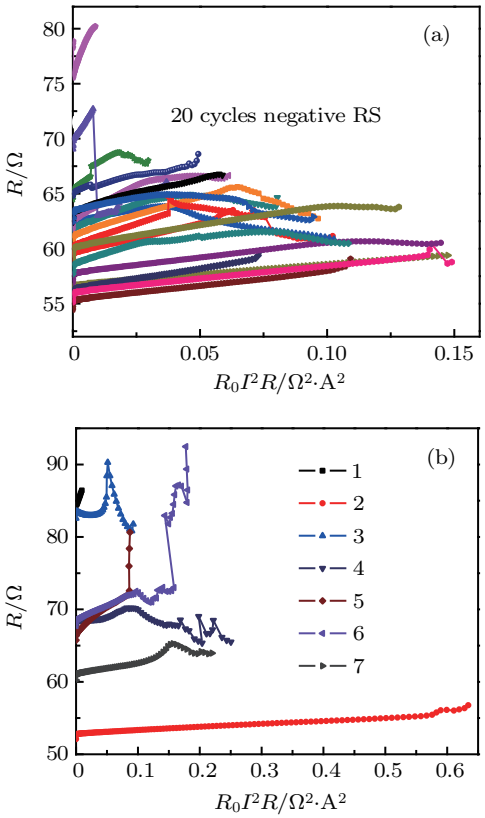


Fig. 5. (color online) Plots for $R(T)$–$R_0I^2R(T)$ of the on state I–V curves. Panels (a) and (b) are corresponding to the curves in Figs. 2(a) and 2(b), respectively.

Now it should be mentioned that the RS behavior of the Au/NiO/Pt cell has been studied. The experimental results show that the RS repeatability is closely related to the working pressure of O_2 gas during the deposition of NiO film. We did not observe the repeated RS behaviors in the NiO film when the O_2 pressure was 12 Pa which is used in this work. So it can be deduced that the repeated RS behaviors observed in the Au/NiO/STO/Pt cell are not caused by the NiO film. In addition, the repeated unipolar RS was observed in the Au/STO/Pt memory cells and was independent of bias polarity in our previous work.[14] According to these comparison results, we have a conclusion that the repeated RS behaviors in the Au/NiO/STO/Pt cell should be caused by the STO film. That is to say, the rupture and rejuvenation of CF occur in the STO film. The STO film is expected to comprise oxygen vacancies, which can be determined by the n-type mate-

rial conduction characteristics according to the unidirectional conduction (as shown in Fig. 2(a)). So, in the set process, filamentary conducting paths, consisting of oxygen vacancies, are formed in STO films as a soft breakdown in the dielectric film and the device switches to LRS. There should be no filaments in the NiO layer because RS behavior is not observed in the Au/NiO/Pt cell. In the reset process, the filaments are disrupted by Joule heat generated by a high current ($I_{\rm reset}$), so that the device returns to HRS.[14]

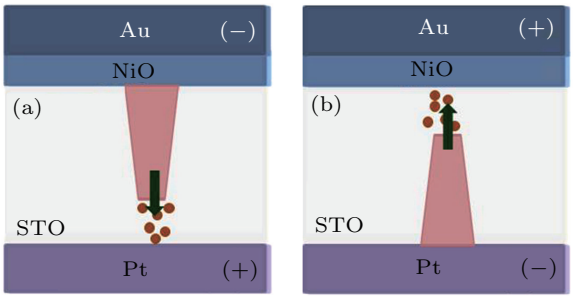


Fig. 6. (color online) Schematic diagrams of the formation and movement of conduction paths composed of oxygen vacancies under (a) negative and (b) positive bias.

Figure 5 and the above analysis show that the switching should occur in different material regions, i.e., in STO film under negative and on the NiO and STO interface under positive bias. So, the unipolar RS depending on the bias polarity should be induced by the movement of the CF ruptured regions according to the bias direction. It is now widely accepted that the CFs in many oxide RS cells do not have a uniform cross-sectional area nor shape along their length direction.[20,21] Furthermore, the origin of RS behavior in STO is caused by oxygen vacancy or ion movement under an applied bias.[22,24–26] The negatively charged oxygen ions move toward the anode under applied bias, and simultaneously oxygen vacancies are created at the cathode and drift toward the anode, forming localized CFs in the oxide. This set process is accompanied with the thickening and thinning of the CFs in the vicinity of the cathode and anode interfaces, respectively. During the following reset process, more Joule heat is generated at the thin CF part by a high $I_{\rm reset}$ due to its large resistance, so the thin CF part is easily ruptured and actually responsible for the switching. Therefore, when a negative bias is applied to the Au/NiO/STO/Pt cell, the oxygen ions will transport from the Au to the Pt, resulting in the conduction paths comprised of oxygen vacancies as shown in Fig. 6(a). The rupture and rejuvenation regions of CFs occur at a weaker CF part near the STO/Pt interface, which results in repeated RS behaviors. When the positive bias is applied to the Au/NiO/STO/Pt cell, the oxygen vacancies generated at the STO/Pt interface would move toward the NiO/STO interface as shown in Fig. 6(b). The reset regions will move towards the weaker CF part. Ultimately, the reset region should be across the NiO/STO interface under positive bias — the corresponding reset curves as shown in Fig. 5(b) take on an abnormal shape with abrupt increase and decrease — which results in the non-switching state. In brief, the RS behaviors of the Au/NiO/STO/Pt cell occur near the anode, which is consistent with the reported results about n-type materials.[27–29] It might be reasonable to assume that an insulating oxide layer without oxygen vacancies is created at the NiO/STO interface. So a non-switching state is observed when positive bias is applied. This can also explain why the resistance of HRS in positive bias is greater than that in negative bias as shown in Fig. 4.

4. Conclusions

In this work, we have fabricated NiO/STO stacked layers using the PLD technique. The unipolar RS properties are observed and its switching repeatability is dependent on the bias polarity. The high resistance in positive bias is greater than that in negative bias. The $R(T)$–$R_0I^2R(T)$ plot of the on state I–V curves shows a regular shape only with a slight bend and an abnormal shape with an abrupt increase and decrease under negative and positive bias, respectively. The unipolar RS properties are caused by the formation and rupture of CFs consisting of oxygen vacancies. The ruptured regions of CFs would move according to the bias direction. Under negative bias, the CFs rupture takes place in the vicinity of the STO/Pt interface, which results in repeated RS behaviors. Under positive bias, the ruptured region moves to the Au anode and ultimately is located at the NiO/STO interface, which results in a non-switching state. This investigation determines the growing direction and rupture location of CF, which will be advantageous to the improvement of the RS cell performances.

References

[1] Liu D Q, Cheng H F, Zhu X, Wang N N and Zhang C Y 2014 *Acta Phys. Sin.* **63** 187301 (in Chinese)
[2] Waser R, Dittmann R, Staikov G and Szot K 2009 *Adv. Mater.* **21** 2632
[3] Yoon J H, Kim K M, Song S J, Seok J Y, Yoon K J, Kwon D E, Park T H, Kwon Y J, Shao X and Hwang C S 2015 *Adv. Mater.* **27** 3811
[4] Shang D S, Sun J R, Shen B G and Wuttig M 2013 *Chin. Phys. B* **22** 067202
[5] Chang S H, Lee J S, Chae S C, Lee S B, Liu C, Kahng B, Kim D W and Noh T W 2009 *Phys. Rev. Lett.* **102** 026801
[6] Chae S C, Lee J S, Kim S J, Lee S B, Chang S H, Liu C L, Kahng B, Shin H J, Kim D W, Jung C U, Seo S, Lee M Y and Noh T W 2008 *Adv. Mater.* **20** 1154
[7] Kwon D H, Kim K M, Jang J H, Jeon J M, Lee M H, Kim G H, Li X S, Park G S, Lee B, Han S W, Kim M Y and Hwang C S 2010 *Nat. Nannotechnol.* **5** 148
[8] Menzel S, Bottger U, Wimmer M and Salinga M 2015 *Adv. Funct. Mater.* **25** 6306
[9] Szot K, Speier W, Gihlmayer G and Waser R 2006 *Nat. Mater.* **5** 312
[10] Kim K M, Song S J, Kim G H, Seok J Y, Lee M H, Yoon J H, Park J and Hwang C S 2011 *Adv. Func. Mater.* **21** 1587
[11] Hu L, Lin G T, Wei R H, Luo X, Tang X W, Zhu X B, Song W H, Dai J M and Sun Y P 2017 *Ceram. Int.* **43** 3177

[12] Lee M J, Lee C B, Lee D, Lee S R, Hur J, Ahn S E, Chang M, Kim Y B, Chung U I, Kim C J, Kim D S and Lee H 2010 *IEEE Electron Dev. Lett.* **31** 725
[13] Hu L, Tang X W, Luo X, Zhang K J, Jin L H, Lin G T, Chen L, Zhu X B, Song W H, Dai J M and Sun Y P 2016 *J. Phys. D: Appl. Phys.* **49** 165308
[14] Sun X W, Li G Q, Ding L H, Yang N and Zhang W F 2011 *Appl. Phys. Lett.* **99** 072101
[15] Ho J K, Jong C S, Chiu C C, Huang C N, Chen C Y and Shih K K 1999 *Appl. Phys. Lett.* **74** 1275
[16] Sun X W, Li G Q, Zhang X A, Ding L H and Zhang W F 2011 *J. Phys. D: Appl. Phys.* **44** 125404
[17] Muenstermann R, Menke T, Dittmann R and Waser R 2010 *Adv. Mater.* **22** 4819
[18] Kim K M and Hwang C S 2009 *Appl. Phys. Lett.* **94** 122109
[19] Lee S B, Chae S C, Chang S H, Lee J S, Park S, Jo Y, Seo S, Kahng B and T W Noh 2008 *Appl. Phys. Lett.* **93** 252102
[20] Kim K M, Kim G H, Song S J, Seok J Y and Lee M H 2010 *Nanotechnology* **21** 305203
[21] Degraeve R, Fantini A, Clima S, Govoreanu B, Goux L, Chen Y Y, Wouters D J , Roussel Ph, Kar G S, Pourtois G, Cosemans S, Kittl J A, Groeseneken G, Jurczak M and Altimime L 2012 *Symposium on VLSI Technology Digest of Technical Papers* pp. 75–76
[22] Lee W, Yoo S, Yoon K J, Yeu I W, Chang H J, Choi J H, Susanne H E, Waser R and Hwang C S 2016 *Sci. Rep.* **6** 20550
[23] Park J, Kwon D H, Park H, Jung C U and Kim M 2014 *Appl. Phys. Lett.* **105** 183103
[24] Lee S, Lee J S, Park J B, Kyoung Y K, Lee M J and Noh T W 2014 *Apl Mater.* **2** 066103
[25] Sun X W, Li G Q, Chen L, Shi Z and Zhang W F 2011 *Nanoscale Res. Lett.* **6** 599
[26] Pan X Q, Shuai Y, Wu C G, Luo W B, Sun X Y, Yuan Y, Zhou S Q, Ou X and Zhang W L 2016 *Appl. Surf. Sci.* **389** 1104
[27] Hwang I, Lee M J, Buh G H, Bae J, Choi J, Kim J S, Hong S, Kim Y S, Byun I S, Lee S W, Ahn S E, Kang B S, Kang S O and Park B H 2010 *Appl. Phys. Lett.* **97** 052106
[28] Yoon K J, Song S J, Seok J Y, Yoon J H, Kim G H, Lee J H and Hwang C S 2013 *Nanotechnology* **24** 145201
[29] Oka K, Yanagida T, Nagashima K, Kanai M, Kawai T, Kim J S and Park B H 2011 *J. Am. Chem. Soc.* **133** 12482